International Journal of Engineering Research and General Science Volume 3, Issue 4, Part-2, July-August, 2015
ISSN 2091-2730

AUTOMATED DETECTION OF SHADOW REGIONS IN HIGH RESOLUTION SATELLITE IMAGES

[1]Mahak Khurana, [2]Vaishali Wadhwa

[1]Mtech. Student, N.C. College of Engineering

[1]Khuranamahak@gmail.com, 09050669567

Abstract— High-Resolution (HR) satellite image is a commanding basis of data for detecting and extracting information about urban constructions. Shadow in HR satellite imageries is capable of providing a high level of detail, which makes them a reliable and highly vital basis of information. Nevertheless, to extract shadows, the automated detection of shadows from images must be perfect. In this paper, we present a global thresholding practice for automated detection of shadow regions from remotely sensed data. This thresholding scheme detects both shadow and vegetation regions of a High Resolution Satellite Image at the same time.

Keywords— High Resolution Satellite Image, Shadow detection, Vegetation mask, Shadow mask, Thresholding, Otsu method, Histogram.

INTRODUCTION

High Resolution (HR) satellite images are one of the most significant data input source to be utilized for the purpose of object detection. However, due to urban constructions which are built above ground, such as buildings, bridges etc., shadows are the most common component accompaniments for these constructions that can be seen in the HR images. A shadow indicates the shape of the object which is casting it.

Satellite images are the type of images that are taken by artificial satellites and contain portion of Earth. In that kind of imagery, image data is captured at specific frequencies across the electromagnetic spectrum. In most cases, the spectral range of satellite images is broader than that of the visible light. In the high resolution (HR) satellite images, the following spectral bands exist with corresponding wavelength intervals:

- Blue: 450 - 515...520 nm
- Green: 515...520 - 590...600 nm
- Red: 600...630 - 680...690 nm
- Near-infrared (NIR): 750 - 900 nm

The existence of NIR band provides valuable information for detecting natural regions and shadows in the satellite image. The satellite image can be visualized by using red, green, blue channels as its standard order (called true-color), as well as mapping NIR, red, green channels to red, green, blue. This is called false-color. This visualization is much useful for identifying vegetative regions. Figure 1.1 shows an example satellite image in true-color and false-color respectively.

For detecting a specific target such as building, road, vehicle, etc; it is essential to obtain a spatial resolution as high as possible. This can be done by a process called pan sharpening.

(a) (b)

Figure 1.1: A satellite image shown in two different visualizations. (a) True color visualization. (b) False color visualization.

Along with the multispectral image data, a single grayscale image, whose spectral resolution is higher than the multispectral image, is also acquired by the optical sensor. This grayscale image is called panchromatic image. The pan sharpening process fuses the high resolution panchromatic image and low resolution multispectral image together to obtain a single high resolution multispectral image. Figure 1.2 shows an example image pan sharpened using a commercial GIS tool called Geoimage:

(a) (b) (c)

Figure 1.3: Pan sharpening process applied on a satellite image. (a) High-resolution panchromatic image. (b) Low-resolution multispectral image. (c) Resulting high-resolution pan sharpened image.

Shadow detection from HR satellite images is not an easy task and all image processing techniques for detecting shadows still rely on the estimation of shadow areas. The reliable and accurate detection of building objects from the HR satellite images is a leading task and is also very active ground of research. The shadow line of the object will be shorter in the case of a rise in a horizontal receiving surface and longer where there is a drop in this surface for the other objects in the urban areas. Also, the subsistence of trees, their shadows and shadows from the non-built-up areas (such as vehicles), can disfigure the real boundaries of shadows (the geometric form such as buildings) and give a random shape to the built-up objects, when they coalesce with an object's shadows. Moreover, the shadow region of an object in image will be larger in the summer season than its equivalent in the winter due to the sun's position in the sky vault and its angle and elevation. Spectrally, non-shadow regions, such as water, generally exhibit the same pixel intensity values or darkness with shadow regions of the objects in images that grounds for an error in detecting shadows.

DETECTION OF VEGETATION AREAS

The pixels corresponding to the vegetation regions have very high reflectance values in the NIR band; while having low reflectance values in the red band. This is because of the emission / absorption characteristics of healthy vegetation. Live green plants need a specific range of solar radiation; between 400 nm 700 nm, to carry on the photosynthesis process. This spectral range is called photo synthetically active radiation and abbreviated as PAR. The wavelength of NIR radiation is longer than 700 nm. Therefore, the radiation with wavelength inside the NIR spectral region is scattered / emitted by the leaf cells; otherwise these rays would overheat and damage the leaves. Hence, healthy vegetation has high reflectance values in NIR spectral region. On the other hand, chlorophyll pigments in leaves absorb the light rays with wavelength equivalent to red, causing red reflectance to have low value. Among these, the most widely used index is Normalized Difference Vegetation Index (NDVI). The formula for calculating NDVI is simply:

$$\boldsymbol{R = (NIR - RIB) / (NIR + RIB)}$$

NIR and *RIB* represent the normalized near-infrared and red image bands, respectively.

For every pixel, the NIR is calculated and an NDVI map is generated for whole image. The decision whether a pixel belongs to a vegetated area or not is made by simply applying Otsu's automatic thresholding method. Figure 2.1 shows an example image of detected vegetation regions in a residential area

It can be seen from its arithmetic characterization that the NDVI of an area containing intense vegetation shade will tend towards the positive values (say 0.3 to 0.8) while clouds and snow fields will be illustrated by the negative values of this index. Further objects on Earth visible from space include:

- free standing water (e.g., oceans, seas, and rivers) which have relatively low reflectance in both shadowlike(spectral) bands and hence, upshot a very low positive or even slightly negative NDVI values, and
- Soils which usually reveal a near-infrared spectral reflectance somewhat greater than the red are inclined to produce somewhat small positive NDVI values (say 0.1 to 0.2).

.

(a) **(b)**

Figure 2.1: Vegetation detection example. (a) Sample image with large vegetation area. (b)Vegetation regions detected using NDVI thresholding.

For every test site, we employ automatic thresholding method to locate the optimum threshold of the histogram of the NDVI ratio values computed from the above equation, and relate that threshold on the NDVI ratio map to compute a binary vegetation mask. To spot the shadow areas, Otsu method is applied to the histogram of the ratio map

DETECTION OF SHADOWS

The approach generates a false color image in which NIR, red and green bands are employed. The algorithm is simple; first, the false color image is normalized and converted to Hue-Saturation-Intensity (ρ_{HSI}) color space. Then, a ratio map (ρ_{RM}), in which the normalized saturation (ρ_S) and the normalized intensity (ρ_I) values are compared with a ratio, is generated:

$$\rho_{RM} = \frac{\rho S - \rho I}{\rho S + \rho I}$$

To detect the shadow areas, as utilized in the case of vegetation extraction, Otsu's method is applied to the histogram of the ratio map, ρ_{RM}. Due to the fact that the thresholding scheme detects both shadow and vegetation regions at the same time, the regions that belong to the vegetation are subtracted to obtain a binary shadow mask. This approach provided successful shadow detection results for various satellite images and the major advantage is that it is independent from manual thresholds. Figure 3.1and 3.2 shows example of detected shadow regions.

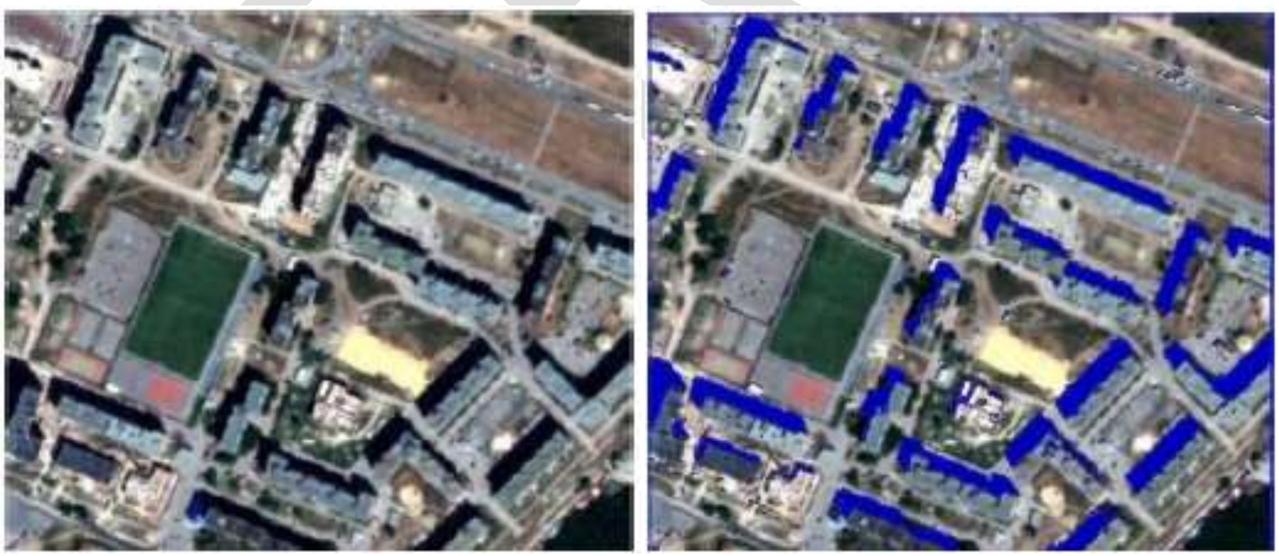

(a) (b)

Figure 3.1: Shadow detection example. (a), Sample image , (b) Shadow detection result

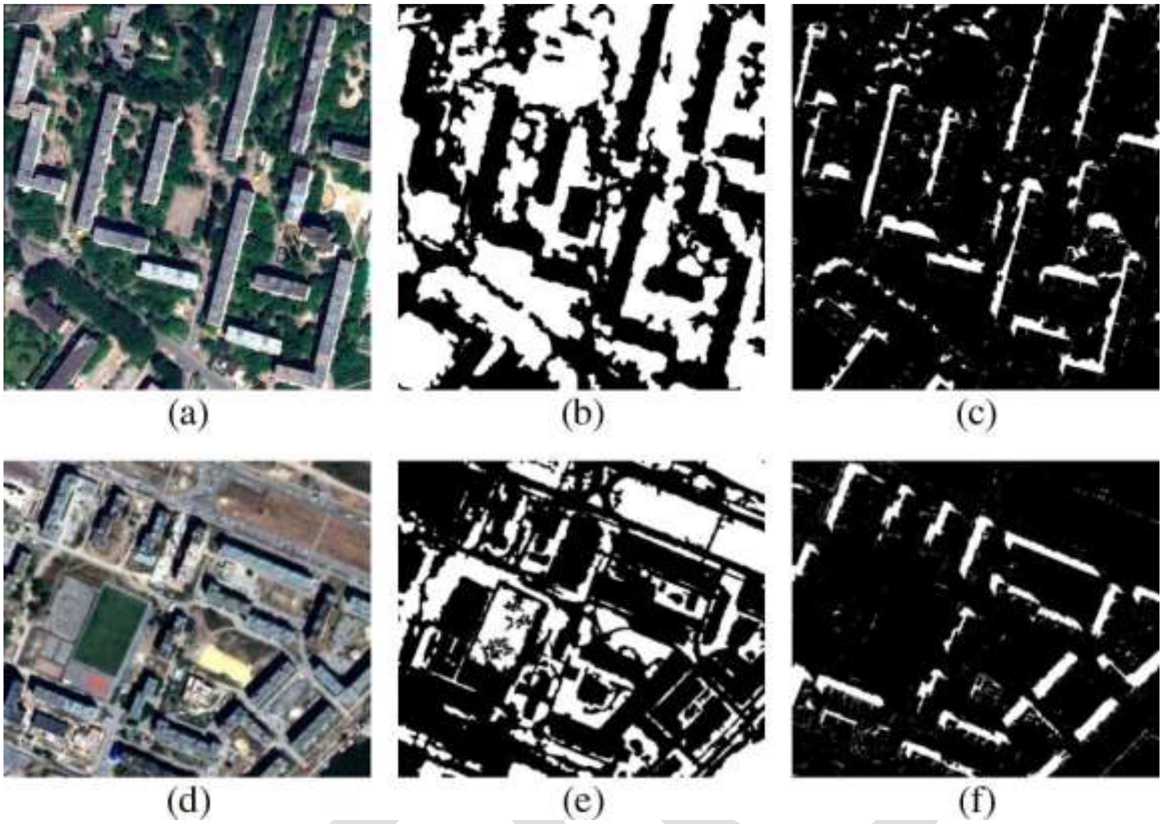

Figure 3.2 :(a), (d) High Resolution satellite image, the generated (b), (e) Vegetation masks and (c), (f) shadow masks

IMAGE THRESHOLDING: OTSU'S THRESHOLDING METHOD

Image thresholding techniques are indispensable in the course of object detection. This is in spite of the verity that the thresholding techniques are a straightforward blueprint for partitioning an image into inaccessible features, they are nonetheless effectual .Alternatively, the thresholding techniques which are applied on HR satellite images for shadow detection are requisite to be more efficient, taking into account the dissimilar characteristics of the worn and old images. As well, the fully automated algorithms of shadow detection regularly call for advance constraining assumptions about extracting shadow regions from HR satellite images in order to run them suitably and acquire reliable exactness of the shadow masks.

In this paper, we bring in, thresholding that is determined to segment the image into two brightness regions which correspond to background and object. Several methods have been proposed to automatically select the threshold. Otsu formulates the threshold selection problem as a discriminant analysis where the gray level histogram of image is divided into two groups and the threshold is determined when the variance between the two groups is the maximum. Even in the case of unimodal histogram images, that is, the histogram of a gray level image does not have two obvious peaks; Otsu's method can still provide satisfactory result.

Thresholding usually involves ***analyzing the histogram***

– Different features give rise to distinct features in a histogram

– In general the histogram peaks corresponding to two features will overlap. The degree of overlap depends on peak separation and peak width.

Otsu is an automatic thresholding method, that automatically selects the best threshold't' in a given Image histogram. It assumes 2 groups are present in the image:

- Those that are <= t.
- Those that are > t.

For *every* possible t:

- Calculate within group variances:
  1. probability of being in group 1; probability of being in group 2
  2. determine mean of group 1; determine mean of group 2
  3. calculate variance for group 1; calculate variance for group 2
  4. calculate weighted sum of group variances
- Remember which t gave rise to minimum.

Otsu's thresholding method is based on selecting the lowest point *between* two *classes* (peaks).

- Frequency and Mean value:

Frequency:

$$\omega = \sum_{i=0}^{T} P(i) \qquad P(i) = n_i / N$$

N: total pixel number

Mean:

$$\mu = \sum_{i=0}^{T} iP(i) / \omega$$

n_i: number of pixels in level i

- Analysis of variance (variance=standard deviation^2)

Total variance:

$$\partial_t^2 = \sum_{i=0}^{T} (i-\mu)^2 P(i)$$

Between-classes variance (δ_b^2):

The variation of the mean values for each class from the overall intensity mean of all pixels:

$$\delta_b^2 = \omega_0 (\mu_0 - \mu_t)^2 + \omega_1(\mu_1 - \mu_t)^2,$$

Substituting $\mu_t = \omega_0 \mu_0 + \omega_1\mu_1$, we get:

$$\delta_b^2 = \omega_0\omega_1(\mu_1 - \mu_0)^2$$

$\omega_0, \omega_1, \mu_0, \mu_1$ stands for the frequencies and mean values of two classes, respectively.

- The criterion function involves *between-classes* variance to the total variance is defined as:

$$\eta = \delta_b^2 / \delta_t^2$$

- All possible thresholds are evaluated in this way, and the one that maximizes η is chosen as the optimal threshold

Matlab function for Otsu's method:

function level = graythresh (I)

GRAYTHRESH compute global threshold using Otsu's method. Level is a normalized intensity value that lies in the range [0, 1].

Now, If **reference value** > **T (i, j),** then **1** at pixel position (referring to the edges of shadows of an object within an image)

Else **0** at pixel position (background image)

Example:

```
>>n=imread ('nodules1.tif');
>> tn=graythresh (n)
tn = 0.5804
>> imshow (im2bw (n, tn))
```

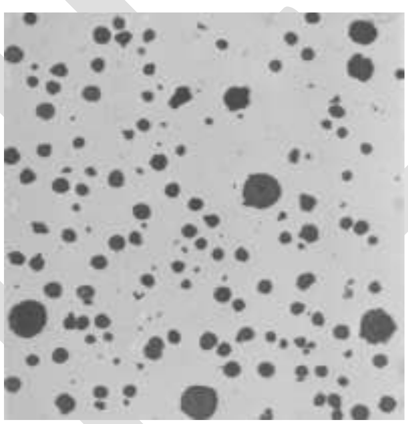

Figure 4.1: Nodules1.tif

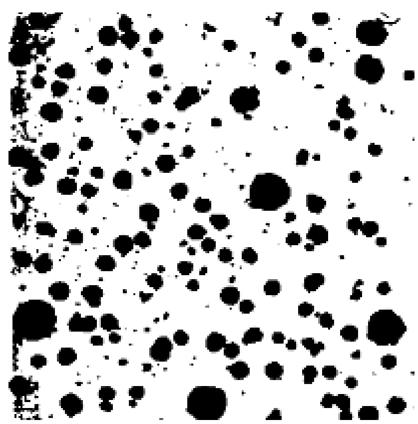

Figure 4.2: Nodules1 after thresholding

ACKNOWLEDGMENT

I want to say thanks to NCCE for the cooperation in completing my work. Specially, I thanks to my guide Ms. Vaishali Wadhwa for her help in performing my Research Paper work and complete it on the time. Without her help I cannot able to complete my work. Last but not least I want to say thanks to my parents who helped me very much and understand my work load.

CONCLUSION

The automated detection of shadows from VHR satellite images is a significant method in applications for building detection, illumination direction analysis from the sun, and the spatial distribution of the object casting the shadow. In this paper, a thresholding technique has been proposed that can handle image with fuzzy boundaries amid the image's object and background. This thresholding scheme detects both the shadow and the vegetation regions of a High Resolution Satellite Image at the same time more reliably and accurately.

REFERENCES:

[1] N. M. Salih M. Kadhim, M. Mourshed, M. T. Bray," *Shadow Detection From Very High Resolution Satellite Image Using Grab cut Segmentation And Ratio-Band Algorithms*", The International Archives of the Photogrammetry, Remote Sensing and Spatial Information Sciences, Volume XL-3/W2, 2015.

[2] D.M. Tsai and Y. H. Chen, "*A fast histogram-clustering approach for multilevel thresholding*," Pattern Recognition Letters, Vol. 13, No. 4, 1992, pp. 245-252

[3] N. Otsu, "*A threshold selection method from gray-level histogram*," IEEE Transactions on System Man Cybernetics, Vol. SMC-9, No. 1, 1979, pp. 62-66.

[4] W. H. Tsai, *"Moment-preserving thresholding: a new approach*," Computer Vision, Graphics, and Image Processing, Vol. 29, 1985, pp. 377-393.

[5] J. C.Yen, F. J.Chang, and S. Chang, "*A new criterion for automatic multilevel thresholding*," IEEE Transactions on Image Processing, Vol. 4, No. 3, 1995, pp. 370-378.

[6] S. Wang and R. Haralick, "*Automatic multithreshold selection,"* Computer Vision, Graphics, and Image Processing, Vol. 25, 1984, pp. 46-67.

[7] P. K. Sahoo, S. Soltani, A. K. C. Wong, and Y. Chen, "*A survey of thresholding techniques*," Computer Vision Graphics Image Processing, Vol. 41, 1988, pp. 233-260.

[8] T. Pun, "*A new method for gray-level picture thresholding using the entropy of the histogram*," Signal Processing, Vol. 2, 1980, pp. 223-237.

[9] J. N. Kapur, P. K. Sahoo, and A. K. C. Wong, "*A new method for gray-level picture thresholding using the entropy of the histogram*," Computer Vision Graphics Image Processing, Vol. 29, 1985, pp. 273-285.

[10] Shabnam Jabari," *Building Detection in Very High Resolution Satellite Image*", ASPRS 2014 Annual Conference Louisville, Kentucky, March 23-28, 2014

[11] J. R. Jensen, *Introductory Digital Image Processing: A Remote Sensing Perspective*. Upper Saddle River, NJ: Prentice-Hall, 2005.

[12] N. Otsu, "*A threshold selection method from gray-level histograms*," Automatic, vol.11, pp. 285–296, 1975.

[13] S. Aksoy, I. Z. Yalniz, and K. Ta¸sdemir, "*Automatic detection and segmentation of orchards using very high resolution imagery,"* IEEE Trans. Geosci. Remote Sens., vol. 50, no. 8, pp. 3117–3131, Aug. 2012.

[14] S. U. Lee and S. Y. Chung, "*A comparative performance study of several global thresholding techniques for segmentation*," Computer Vision Graphics Image Processing, Vol. 52, 1990, pp. 171-190.